Surface Shape Reconstruction of a Nonrigid Transparent Object Using Refraction and Motion

Hiroshi Murase

Abstract—**The appearance of a pattern behind a transparent, moving object is distorted by refraction at the moving object's surface. This paper describes an algorithm for reconstructing the surface shape of a nonrigid transparent object, such as water, from the apparent motion of the observed pattern. This algorithm is based on the optical and statistical analysis of the distortions. It consists of the following parts: 1) extraction of optical flow, 2) averaging of each point trajectory obtained from the optical flow sequence, 3) calculation of the surface normal using optical characteristics, and 4) reconstruction of the surface. The algorithm is applied to both synthetic and real images to demonstrate its performance.**

Index Terms—**Computer vision, image recovery, motion analysis, optical flow, surface reconstruction.**

I. Introduction

One of the primary tasks of a computer vision system [1] is to capture 3-D information, such as surface orientation, from 2-D images. This task is usually difficult. However, if some cues are known about the scene, such as stereopsis (e.g., [2], [3]), shading (e.g., [4], [5]), contour (e.g., [6], [7]), texture (e.g., [8], [9]), and motion (e.g., [10]–[18]), 2-D images may provide information about the surface. This information is first converted into local surface orientation [19] and then into the shape of the surface. This correspondence proposes a method for reconstructing the surface shape of an undulating transparent object, such as a water surface, using the cues of refraction and motion. Surface orientation is made from the moving (apparent distortion) of patterns viewed through the object. This approach is similar to the method called shape from motion. The previous work in shape from motion involves reconstructing a 3-D structure from movement of several points on the object based on an assumption of rigidity (e.g., Ullman *et. al.* [10]–[17]). The method described in this paper does not use the rigidity assumption but uses physical characteristics such as optical laws and statistical motion features of the object. In addition, the method uses points on refracted images rather than points on the object.

In this method, the objects should have the following two characteristics: 1) They should be transparent with a refraction index not equal to unity, and 2) their surface shape should be deformed around an average surface whose shape is known. To clarify the essence of the idea, an example of a water surface with waves [20], [21], like the surface of a pool or river, is used. Because of refraction at the water surface, the observed pattern of objects under water with waves appears to be moving. Note that human beings can perceive the surface shape from the observed moving pattern. In this case, the above two characteristics correspond to the following: 1) Water is transparent and has a refraction index of 1.33; 2) the average surface is usually a plane whose surface normal is vertical, and a wave can be regarded as a deformation from the average shape. The goal here is to reconstruct the shape of the water surface from deformed images observed through the waving water and, in so doing, recover the original pattern under the water. The original pattern under the water is assumed to be unknown.

This method has two main original ideas. First, it can be considered to be the inverse operation of the ray-tracing approach. The ray-tracing technique is a common method in the field of computer graphics. It is based on an optical law such as a refraction law (Snell's law) or a reflection law and is used to synthesize the images from the given model (shapes of the objects). For example, Ts'o [22] synthesized ocean wave images using physical characteristics and ray-tracing techniques.

Second, this method uses the idea that the pattern observed through the undulating surface is deformed around the pattern observed through the average surface. In the simplest case of the top view and orthographic projection, the average coordinate of the trajectory of a certain point on the distorted pattern corresponds to the the point observed through the static flat water surface. This means that the average position of the point becomes the position observed when there is no water.

The algorithm consists of the following four parts:

1) Optical flow is calculated from an image sequence observed through the moving water surface. Here, "optical flow" refers to point-to-point correspondence between two succeeding image frames. A trace of the optical flow becomes the trajectory of

Manuscript received January 3, 1990; revised February 3, 1992. Recommended for acceptance for by Associate Editor N. Ahuja.

The author is with NTT Basic Research Labs, Tokyo, Japan.

IEEE Log Number 9200155.

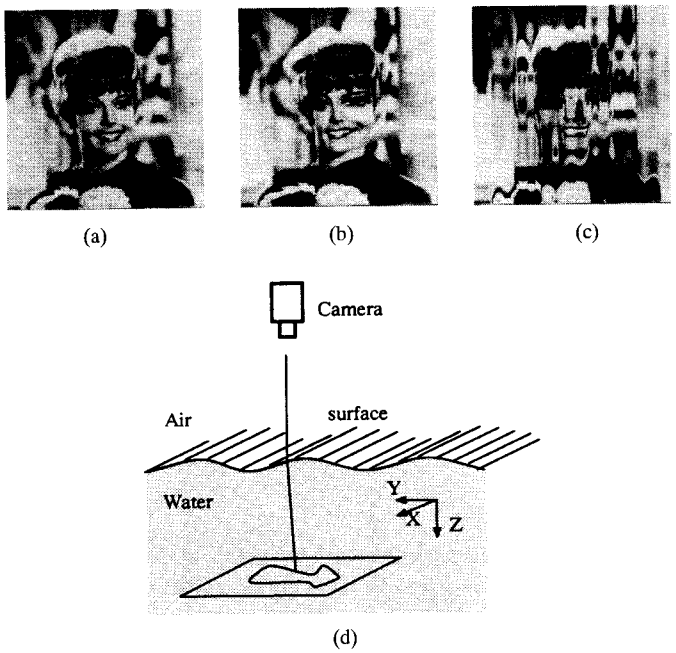

Fig. 1.(a) Original pattern; (b) pattern observed through water with a smooth wave; (c) pattern observed through water with a steep wave; (d) observation system.

the point.

2) The average of the trajectory of the each point in the image is calculated; we call this the center of trajectory (COT). The COT corresponds to the point observed through the average surface.
3) The surface normal of each point in each frame is calculated using optical characteristics. The distance between the COT and the position of the corresponding point in the image is restricted by the optical law (Snell's refraction law), and it is related to the surface normal.
4) The shape of the surface at each point in time can be reconstructed by 2-D integration of the surface normal.

This kind of algorithm offers several new possibilities. For example, a transparent object's shape can be passibly measured, and quality pictures can be taken through transparent undulating objects.

The organization of the paper is as follows. Section II introduces the object treated and summarizes the necessary assumptions. Section III summarizes the relevant optical characteristics. Section IV explains the algorithm, using synthesized images, which reconstructs the shape of the nonrigid surface and recovers the bottom pattern from the distorted image sequence. Section V describes the application of the method to natural images. Finally, an error estimate for the method is computed.

II. Object

First, a brief example is presented. Fig. 1(a) is an image from the image database SIDBA distributed by Tokyo University. Let us assume that the image is put at the bottom of a pool with waving water like Fig. 1(d). The pattern seen through the water would be distorted and would look, for example, like Fig. 1(b) for a smooth wave and like Fig. 1(c) for a steep wave. The purpose of our study is first to reconstruct the wave shape from a time series of distorted patterns and finally to detect the original pattern of Fig. 1(a).

A. Conditions

To make the problem tractable, the following three conditions were introduced:

1) The amplitude of the wave is small enough that elimination or separation of the pattern does not occur in the observed images (i.e., Fig. 1(b)). Fig. 1(c) is an example containing elimination and separation; therefore, it is beyond the scope of our research at present.
2) The camera is far from the object (orthographic projection).
3) All points in the image are in focus (pin hole camera).

B. Assumptions

The following three assumptions are made in the method. Note that the assumption of periodic movement or periodic shape of the surface is not used:

1) The average slant of the wave surface over a long time period is zero.
2) Water is transparent and refractive.
3) The pattern in the water is static and flat.

C. Known Parameter

The following parameters, if known, allow the precise surface shape to be determined. If these are not known, the surface shape may still be determined within a scale factor:

1) Distance h between the water surface and the bottom of the tank
2) refraction index n of water.

III. Relation Between Displacement and Surface Orientation

Fig. 2(a) is a picture of a rigid transparent sphere on a checker pattern, and (b) is a picture of a pond with waves. We can perceive the refractive sphere in Fig. 2(a). In this case, it is assumed that the background pattern is regular. This case represents the problem of reconstructing the shape of a rigid transparent medium atop a known static pattern. On the contrary, we cannot perceive the waving water (only scattered stones) in the static picture of Fig. 2(b) because the background pattern is irregular (the background pattern is unknown). If dynamic images are provided, however, we could perceive the water very clearly. This case represents the problem of reconstructing the shape of a nonrigid transparent medium atop an unknown static pattern. In this situation, we unconsciously use several assumptions like those in Section II, especially the assumption of nonrigid motion around the average surface (see assumption 1) in the previous section). This problem is treated in this paper. In the waving water example, the only physical assumptions introduced are that water is a transparent substance with a certain refraction index and that the average slant of waves in a long time scale converges to zero. When a stone falls into water or the wind blows, a complex pattern is generated on the water surface. These wave patterns are generally complicated due to the governing fluid dynamics. To keep the application areas as broad as possible, additional assumptions regarding dynamic behavior have not been introduced, and in fact, such assumptions are not necessary for the problem of Section II.

A. Optical Characteristics

The refraction law, which is generally known as Snell's law, is effective for this problem with respect to several optical characteristics such as refraction, reflection, polarization, and color dispersion. The principle theory of the method based on the refraction law is illustrated in Fig. 3. Assuming orthographic projection, a small area of the image, which is located at P, is observed to be at Q due to refraction at the water surface. Here, Snell's law is expressed by the vector equation

$$n\vec{r} - \vec{s} = \vec{N}(n\cos b - \cos a) \tag{1}$$

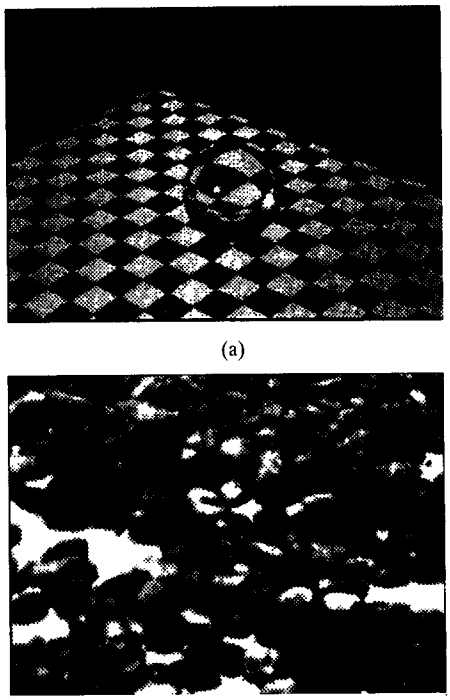

(a) (b)

Fig. 2. Shape perception of transparent objects: (a) Rigid transparent sphere; (b) pond with waving water.

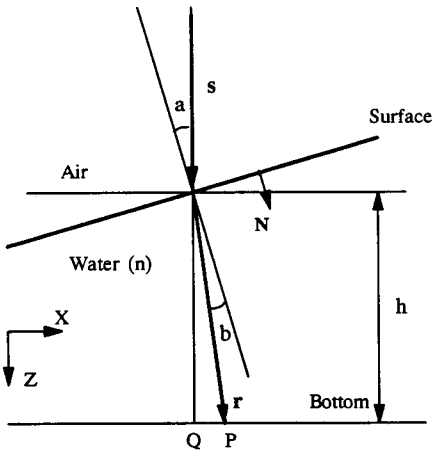

Fig. 3. Optical law of refraction.

where n is the refraction index, $\vec{N}$ is the surface normal, $\vec{s}$ is a unit vector of the ray in air, $\vec{r}$ is a unit vector of the ray in water, a is the incident angle, and b is the refractive angle. The deformation vector $\vec{D}$ is given by

$$\vec{D} = \frac{h\vec{r}}{(\vec{z}, \vec{r})} - h\vec{z}. \tag{2}$$

For the case of orthographic projection, the displacement $\vec{D}$ shows the difference between the position of a point on the observed image and the position on the underwater image. In other words, the observed image is distorted because of the displacement $\vec{D}$.

In order to solve these simultaneous vector equations for $\vec{D}$ using (1) and (2), the unknown vector variables are replaced by the following variables:

$$\vec{s} = (0, 0, 1) \tag{3}$$

$$\vec{r} = (r_x, r_y, r_z) \tag{4}$$

here

$$r_x^2 + r_y^2 + r_z^2 = 1 \tag{5}$$

$$\vec{z} = (0, 0, 1) \tag{6}$$

$$N = \frac{(p, q, 1)}{k} \tag{7}$$

here

$$k^2 = p^2 + q^2 + 1 \tag{8}$$

$$\vec{D} = (d_x, d_y, 0). \tag{9}$$

Here, vector $\vec{s}$ can be expressed by (3) because of the assumption of orthographic projection.

If we rearrange the above equations, d_x and d_y are given by the following equations:

$$d_x = hp\frac{\sqrt{n^2 - k^2 + 1} - 1}{\sqrt{n^2 - k^2 + 1} - 1 + k^2} \tag{10}$$

$$d_y = hq\frac{\sqrt{n^2 - k^2 + 1} - 1}{\sqrt{n^2 - k^2 + 1} - 1 + k^2}. \tag{11}$$

The vector (p, q) is gradient of the surface. k is a weight for normalizing the surface normal $\vec{N}$.

Provided that $k \approx 1$, the water surface is quiet enough. The equations under these conditions are approximated by

$$d_x = hp(1 - \frac{1}{n}) \tag{12}$$

$$d_y = hq(1 - \frac{1}{n}). \tag{13}$$

B. Statistical Characteristics

It is an appropriate assumption regarding water that the average surface normal converges to a vertical line as time passes. This statistical characteristic comes from the motion randomness of the waving water; it can be explained by the following. Typical wave patterns, for example, appearing on a pool surface can be assumed to be superposed patterns of sine waves with different wave lengths and wave speeds. Such wave patterns can be expressed by

$$f(x, y, t) = \sum_i a_i \sin(u_i x + v_i y - w_i t) \tag{14}$$

where (u_i, v_i) is the wavenumber, w_i is the angular frequency, a_i is the amplitude, and $f(x, y, t)$ is the wave height at position (x, y) and time t. The surface normal $\frac{(p,q,1)}{k}$ at a certain point (x, y) can be obtained from the following equations for p and q

$$p = -\frac{\partial f}{\partial x} = -\sum_i a_i u_i \cos(u_i x + v_i y - w_i t) \tag{15}$$

$$q = -\frac{\partial f}{\partial x} = -\sum_i a_i v_i \cos(u_i x + v_i y - w_i t). \tag{16}$$

Thus, average values p' and q', with respect to time, of p and q are expressed by

$$p' = \frac{1}{T}\int_0^T p dt \tag{17}$$

$$q' = \frac{1}{T}\int_0^T q dt. \tag{18}$$

Assuming that w_i is never equal to zero, p' and q' will converge to zero as T increases. In special situations, such as a continuous spout of water, w_i in (17) and (18) can be zero. In such a case, p' and q' would not converge to zero, and the accuracy of the shape reconstruction would be reduced.

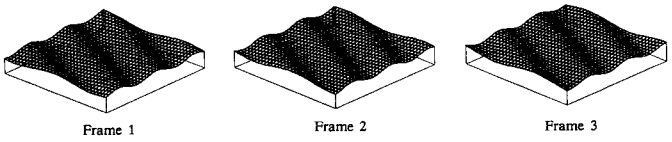

Fig. 4. Sequence of wave surface shape for synthesizing images.

Fig. 5. Synthesized image sequence distorted by refraction.

IV. Reconstruction Algorithm

A. Outline of the Algorithm

The purpose of the algorithm is to reconstruct the shape of the water surface and to detect the image under the water. It consists of the following four steps: 1) extraction of optical flow, 2) averaging the trajectory of each point in the observed images, 3) calculation of the surface slant using optical characteristics, and 4) shape reconstruction. Each step is detailed in the following experiments using synthesized images.

B. Synthesized Image

Synthesized images were used to demonstrate the method. The images were synthesized by the ray-tracing method. Let us look at one of the examples. Let the pattern of Fig. 1(a) (50 × 50 cm) be an underwater pattern. The depth of the water is 50 cm. The sine wave moves diagonally from the upper left of the image to the lower right along the water surface. The maximum slant is 5.0°, the wavelength is 16.6 cm (three cycles in 50 cm), and the wave speed is 2.1 cm/frame (eight frames = one cycle). Fig. 4 shows a sequence of wave surface shapes for synthesizing images (frames 1, 2, and 3). The viewing point is high enough that the projection can be approximated as orthographic. Fig. 5 shows dynamic images (frames 1, 2, 3, and 4) obtained by this method. In this case, the surface shape is periodic. However, the algorithm can also reconstruct a water surface that is not clearly periodic.

C. Extraction of Optical flow

Optical flow expresses the movement of a certain point in the images from one time to another. The optical flow vector at a point corresponds to the speed and direction of motion at that point. For computation, the gradient method (e.g., [23]), the correlation method (e.g., [24]) and the token tracking method are well known. Various methods were used for various patterns. The correlation method,

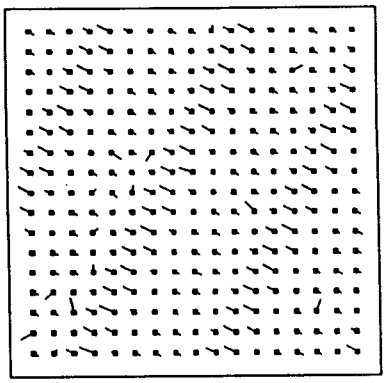

Fig. 6. Extraction of optical flow.

which is a simple algorithm, is applied to these synthesized images since correlative features are preserved throughout the series of images at different frames in the experiment. The correlation value $d(i',j')$ between the rectangle (with side length a) nearest to (i,j) in the tth frame and the rectangle nearest to $(i+i',j+j')$ in the $(t+1)$th frame is determined from the following equation:

$$d(i',j') = \sum_{\frac{-a}{2}<k,l<\frac{-a}{2}} \left| f(i+i'+k, j+j'+l, t+1) - f(i+k, j+l, t) \right|. \quad (19)$$

The vector (i',j') that makes $d(i',j')$ smallest is considered to be the optical flow of (i,j) at time t. Fig. 6 shows an example of an optical flow map extracted by this method.

D. Center of the Trajectory (COT)

In this section, we define COT, which is the main point of the algorithm, and we suggest a method that uses COT to recover the underwater pattern, which is the second purpose of this paper. Consider a certain point P_t in the observed image at time t. The trajectory of P_t is derived from the optical flow. Here, the trajectory is neither separated nor eliminated because of the assumption that the amplitude of water is small. The average coordinate (x,y) of the trajectory of P_t is defined as the COT of point P_t. This corresponds to the position of P_t, whose surface has an average shape with time. The average surface normal generally converges to zero (horizontal flat surface). In most cases, the convergence can be detected when $|\mathrm{COT}_{(\mathrm{using} P_1, P_2, \ldots, P_t)} - \mathrm{COT}_{(\mathrm{using} P_1, P_2, \ldots, P_{t+1})}|$ is less than some threshold for all points.

Fig. 7(a) shows the obtained COT's of periodically placed points at a certain frame of the above synthesized images, whereas Fig. 7.(b) shows the theoretically correct COT's.

The underwater pattern can be recovered by using the COT. The image obtained by mapping all pixels of an observed image at a certain time on their corresponding COT will be the image as seen through a flat water surface if orthographic projection can be assumed. The recovered image of a synthesized sequence is shown in Fig. 8. The remaining distortion in this image is only due to incorrect extraction of optical flow.

E. Gradient Vector Field

If the points (x_t, y_t) and COT (x', y') of a point are known, the direction of the vector normal to the water surface (p_t, q_t) at (x_t, y_t) can be calculated from (12) and (13). The gradient at (x_t, y_t) is thus obtained from

$$P_t = \frac{(x_t - x')n}{h(n-1)} \quad (20)$$

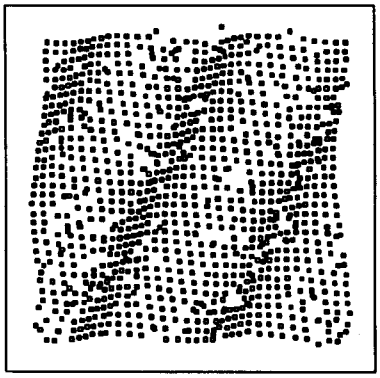

(a)

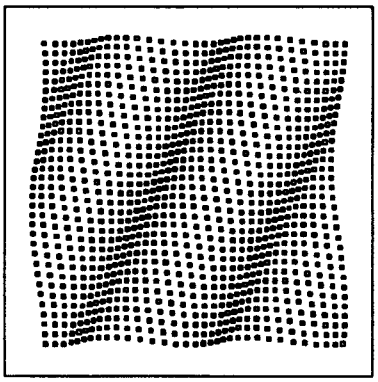

(b)

Fig. 7(a). Calculated center of trajectory; (b) theoretically correct center of trajectory.

Fig. 8. Recovered underwater pattern.

$$q_t = \frac{(y_t - y')n}{h(n-1)}. \tag{21}$$

It requires a large amount of computation to extract the optical flow vector for all points in the image. Therefore, optical flows, COT's, and gradient vectors are first computed corresponding to the selected points, and the gradient vector of each pixel is calculated by averaging the gradient vector of four points adjacent to the pixel. Gradient vectors of different points in image frame 1 are shown in Fig. 9. Here, the vectors are thinned out for clarity. This figure is also called the needle map.

F. Shape Reconstruction

When the gradient vectors of each point are given, the surface shape can be reconstructed by integrating them over the X and Y dimensions. The reconstructed surface shapes for frames 1, 2, and 3 are illustrated in Fig. 10. The Z direction has been expanded for clarity.

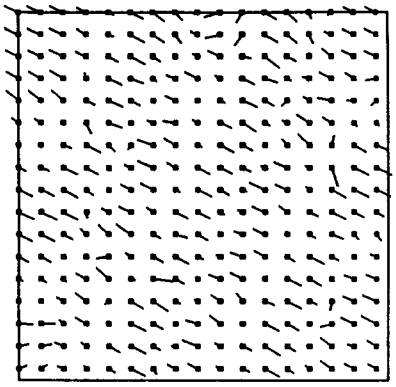

Fig. 9. Vector field showing surface normal.

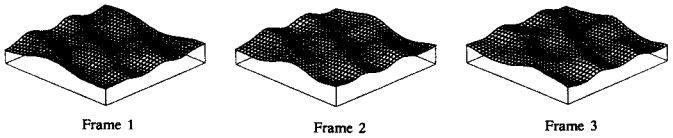

Fig. 10. Shape reconstruction of wave surface.

V. Experiment with Real Images

A. Collecting Data

A TV camera was used to collect data. First, 2 × 2 mm black dots were randomly scattered on a blank sheet of paper by a computer. The paper was fixed on the bottom of a water tank with a water depth $h = 25$ cm. This situation is similar to the one where black stones are scattered randomly in a pond. Waves were then induced by stirring the water. A video camera was placed 1 m from the water surface. The camera produced an image of 512 × 480 pixels, and the focal length was fixed so that one pixel on the sampled image corresponded to 0.5 × 0.5 mm on the underwater pattern. Ninety frames of dynamic images were collected at a rate of 30 frames/s for 3 s. We applied the algorithm to the black dot pattern because this case is relatively simple for optical flow extraction. Application of the algorithm to continuous shading images in a real situation is a problem that will be dealt with later.

B. Preprocessing

In the case of actual images, shading occurs due to the camera's characteristics, imbalanced illumination, light refraction at the water surface, and so on. Therefore, prior shading correction is necessary. We made images with large-radius Gaussian filters for each frame. We took the average of the 30 images and produced a shading correction image. Desired images were then generated by subtracting the shading correction image from the original images. Figs. 11(a) and (b) are examples of original images (frames 1 and 2), (c) is an example of a shading image, and (d) is the corrected image of frame 1.

C. Extraction of Optical Flow

For these images, black pixel clusters are useful tokens for optical flow extraction. The process based on the token tracking method is as follows. First, the shading corrected images are binarized, and then, parts having more than a specified number of black pixels are picked up. The optical flow is extracted by tracing these parts. The optical

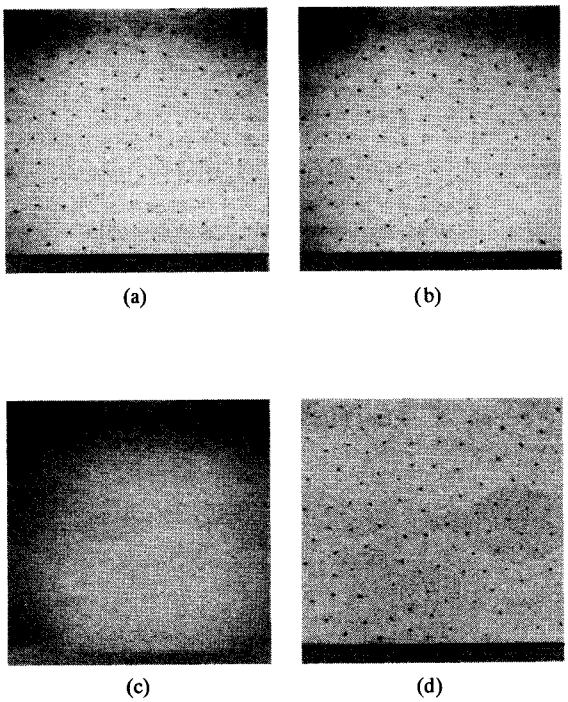

Fig. 11. (a), (b) Observed image sequence (frames 1 and 2); (c) shading image; (d) image of the corrected shading (frame 1).

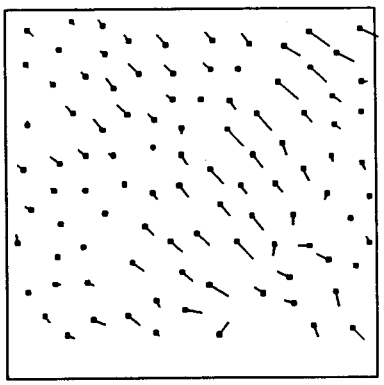

Fig. 12. Optical flow.

flow obtained by this method was manually checked and found to contain no errors. Fig. 12 is an optical flow map extracted from frame 6.

D. Determination of COT

Fig. 13 shows the trace of a certain point on the image for 0.66 s (20 frames) using optical flow. From this result, it can been seen that the locus of a point moves around a certain point of the real image. The COT can be calculated in the same way as explained in Section IV-D. Fig. 14 shows calculated COT's and the actual pattern of black points located at the bottom of the water.

E. Computation of Gradient Vector Field

The gradient vector field was calculated using the positional relation between a point and its COT, as explained in Section IV-E. As an example, the gradient vector field for frame 6 is shown in Fig. 15.

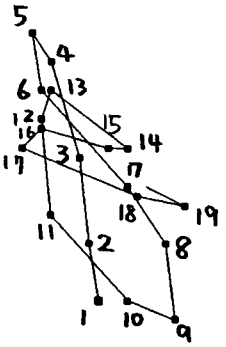

Fig. 13. Tracking of a point of a pattern.

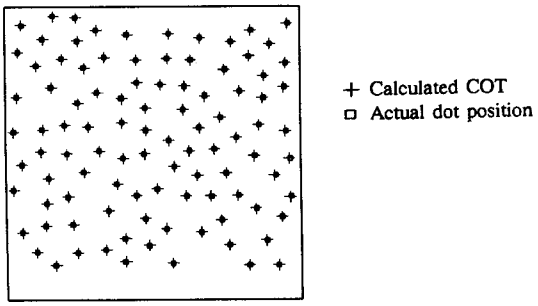

Fig. 14. Center of trajectory.

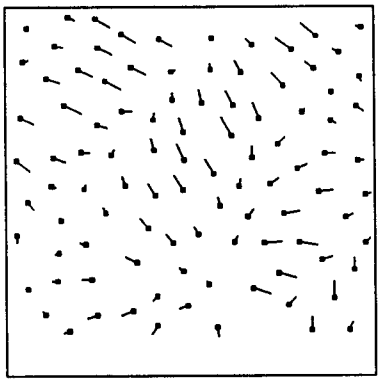

Fig. 15. Vector field showing surface normal.

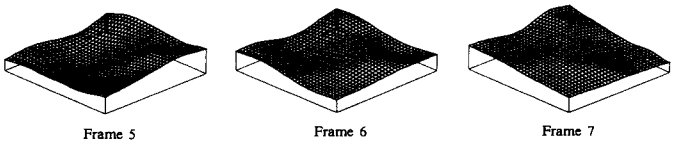

Fig. 16. Sequence of reconstructed surface shape.

F. Shape Reconstruction

The shape of the wave was reconstructed from the gradient vector field using the method of Section IV-F. Fig. 16 shows the sequence of reconstructed surface shapes for frames 5 through 7. Thus, it has been demonstrated that the wave shape can also be reconstructed for a real image sequence. Therefore, the algorithm presented here is useful for shape reconstruction in a passive observation system.

VI. Shape Reconstruction Errors

Errors in shape reconstruction are evaluated in this section. The errors are mainly due to 1) failure in extracting optical flow and

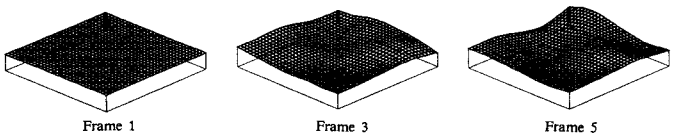

Fig. 17. Surface shape reconstruction using only the first N frames.

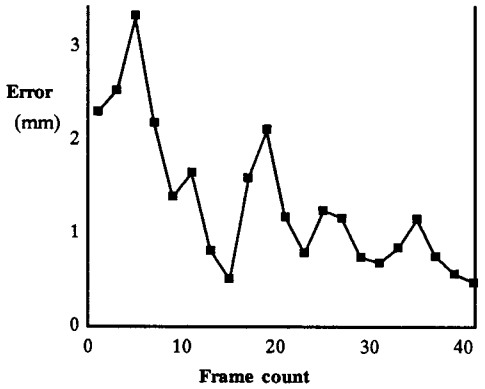

Fig. 18. Estimated errors of the surface shape reconstruction.

2) errors in calculating COT. To improve 1), a better calculation algorithm needs to be developed. Here, we concentrate on the evaluation of errors 2). Errors can be minimized by prolonging the time used for the extraction of optical flow. Results are presented below for experiments with real images that were conducted in order to evaluate the errors.

We assume that the available information for calculating COT is taken from the first frame ($t = 1$) through the present frame. The present frame shows the frame whose shape is to be reconstructed. The same data stated in Section V are used here. Examples of reconstructed wave shapes are given in Fig. 17. As is apparent from Fig. 17, a flat shape for the first frame is obtained because the COT coincides with that point, and no gradient is detected. As the number of analyzed frames increases, however, the shape becomes clearer. For example, the shape for frame 5 is more apparent than that for frame 3. This means that the errors decrease as more frames are used for the shape reconstruction.

The error in the tth frame S_t is defined as

$$S_t = \frac{1}{M} \sum_{i,j} |Z_{tij} - Z'_{tij}| \tag{22}$$

where M is the total number of combinations of i and j, Z_{tij} is the Z value at coordinate (i, j) at the tth frame of the reconstructed shape by our method, and Z'_{tij} is the Z value of the actual surface shape. The actual surface shape is calculated using the real positions of the underwater dot pattern. As shown in Fig. 18, the error decreases with repeated oscillation. The phenomenon of increasing error during the first few frames can be explained as follows. The position of points tends to oscillate; therefore, some points move in a different direction from the COT. Where such points predominate, the error first increases but then decreases after a long period.

The algorithm for recovery of the underwater patterns also uses COT. Accordingly, the deformation of the recovered pattern gradually decreases with time.

VII. Conclusions

The movement of a transparent object past a pattern distorts the observed image of the pattern. This correspondence dealt with the surface shape reconstruction of transparent objects from a sequence of distorted 2-D images. The reconstruction can be thought of as an inverse operation of the ray-tracing technique, which is well known in computer graphics. The proposed method can deal with objects having the following characteristics: 1) They are transparent with a nonunity refraction index, and 2) their surface shapes are deformed around an average surface whose shape, in relation to time, is known. Its originality lies in dealing with a nonrigid transparent object and in using cues of refraction (optical law, which is the above characteristic 1)) and motion (statistical characteristics of the object, which is the above characteristic 2)). An example of a waving water surface was used to demonstrate the method.

The main results of this correspodence are listed below:

1) The gradients of each point of the transparent object (for example, water surface), which is referred to as a needle map, can be computed from the positional relation between the point and its COT, even if the original pattern is unknown. The surface shape can be reconstructed by integration of this gradient map. This has been demonstrated in experiments using both synthesized and real images of an image behind water.
2) The original pattern can be recovered from the time series of the distorted images. Distortion is corrected by inversely transforming each pixel to its COT. An example of original pattern recovery was demonstrated using a synthesized image sequence.
3) The error caused by estimation error of the COT, even if it first increases, decreases as time passes.

Areas for future research include improving the accuracy of optical flow extraction, developing the case of center projection, and applying the method to various kinds of real images.

Acknowledgment

The author would like to thank Dr. S. Naito and Dr. R. Nakatsu for their valuable advice and encouragement. He is also grateful to Mrs. Y. Murase for her linguistic collaboration.

References

[1] H. Ballard and C. M. Brown, *Computer Vision*. Englewood Cliffs, NJ: Prentice-Hall, 1982.
[2] W. E. L. Grimson, *From Images to Surfaces, A Computational Study of the Human Early Visual System*. Cambridge, MA: MIT Press, 1981.
[3] B. Julesz, "Binocular depth perception of computer-generated patterns," *Bel Syst. Tech. J.*, vol. 39, pp. 1125–1162, 1960.
[4] B. K. Horn, *Robot Vision*. Cambridge, MA: MIT Press, 1986.
[5] K. Ikeuchi and B. K. P. Horn, "Numerical shape from shading and occluding boundaries," *Artificial Intell.*, vol. 17, pp. 141–184, 1981.
[6] M. Brady and A. Yuille, "An extremum principle from shape from contour," *IEEE Trans. Patt. Anal. Machine Intell.*, vol. PAMI-6, pp. 288–301, 1984.
[7] A. P. Witkin, "Recovering surface shape and orientation from texture," *Artificial Intell.*, vol. 17, pp. 17–45, 1981.
[8] K. A. Stevens, "The visual interpretation of surface contours," *Artificial Intell.*, vol. 17, pp. 47–74, 1981.
[9] J. Aloimonos, "Shape from texture," *Biol. Cybern.*, vol. 58, pp. 345–360, 1988.
[10] H. C. Longuet-Higgins, "The visual ambiguity of a moving plane," in *Proc. Roy. Soc. London Ser. B*, vol. 223, pp. 165–175, 1984.
[11] R. Y. Tsai and T. S. Huang, "Uniqueness and estimation of three-dimensional motion parameters of rigid objects with curved surfaces," *IEEE Trans. Patt. Anal. Machine Intell.*, vol. PAMI-6, pp. 13–27, 1984.
[12] M. Subbaro "Interpretation of image flow: Rigid curved surface in motion," *Int. J. Comput. Vision*, vol. 2, pp. 77–96, 1988.
[13] K. Sugihara and N. Sugie, "Recovery of rigid structure from orthographically projected optical flow," *Comp. Vision Graphics Image Processing*, vol. 27, pp. 309–320, 1984.
[14] K. Kanatani "Structure and motion from optical flow under perspective projection," *Comput. Vision Graphics Image Processing*, vol. 38, pp. 122–146, 1987.

[15] H. -H. Nagel, "Representation of moving rigid objects based on visual observations," *IEEE Comput.*, vol. C-14, pp. 29–39, 1981.
[16] O. D. Faugeras, F. Lustman, and G. Toscani, "Motion and structure from motion from point and line matches," in *Proc. First Int. Conf. Comput. Vision* (London, UK), 1987, pp. 25–34.
[17] S. Ullman, *The Interpretation of Visual Motion*. Cambridge, MA: MIT Press, 1979.
[18] J. J. Gibson, *The Ecological Approach to Visual Perception*. Boston, MA: Houghton Mifflin, 1979.
[19] D. Marr, *Vision*. New York: W. H. Freeman, 1982.
[20] B. L. Gotwols and G. B. Irani, "Charge-coupled device camera system for remotely measuring the dynamics of ocean waves," *Appl. Opt.*, vol. 21, no. 5, pp. 851–860, Mar. 1982
[21] B. Jahne, "Image sequence analysis of complex physical objects: Nonlinear small water surface waves," in *Proc. 1st Int. Conf. Comput. Vision*, 1987, pp. 191–200.
[22] P. Y. Ts'o and B. A. Brasky, "Modeling and rendering waves: Wave-tracing using beta-splines and reflective and refractive texture mapping," *ACM Trans. Graphics*, vol. 6, no. 3, pp. 191–214, July 1987.
[23] B. K. P. Horn, "Determining optical flow," *Artificial Intell.*, vol. 17, pp. 185–203, 1981.
[24] J. M. Prager and M. A. Arbib, "Computing the optic flow: The MATCH algorithm and prediction," *Comput. Vision Graphics Image Processing*, vol. 24, pp. 213–237, 1984.